Revista Mexicana de Astronomía y Astrofísica, **46**, 279–290 (2010)

SPECTRAL VARIABILITY OF ROMANO'S STAR

O. Maryeva,[1, 2] and P. Abolmasov[3]

Received 2010 February 3; accepted 2010 June 10

RESUMEN

Combinamos observaciones espectroscópicas de archivo de la estrella LBV V532 (conocida como Estrella de Romano) con fotometría en la banda B. Los datos espectroscópicos cubren un intervalo de 15 años, desde 1992 hasta 2007. Mostramos que en máximo de brillo el objeto se comporta como una supergigante con líneas de emisión, mientras que en mínimo V532 se mueve a lo largo de la secuencia de las estrellas WN tardías. En este sentido, la estrella tiene un comportamiento similar al de las bien conocidas variables luminosas azules (LBV: luminous blue variables) AG Car y R 127, pero es un poco más caliente en mínimo. Identificamos unas 100 líneas espectrales en el intervalo 3700–7300 Å. Nuestra espectroscopía para este objeto es la más completa en la actualidad. Obtenemos la velocidad del viento usando las líneas del triplete de He I (300 ± 30 km s^{-1}). También estimamos los parámetros físicos de la nebulosidad que rodea a V532.

ABSTRACT

We combine archival spectral observations of the LBV star V532 (Romano's star) together with existing photometric data in the B band. Spectroscopic data cover 15 years of observations (from 1992 to 2007). We show that the object in maximum of brightness behaves as an emission line supergiant while in minimum V532 moves along the sequence of late WN stars. In this sense, the object behaves similarly to the well-known Luminous Blue Variable (LBV) stars AG Car and R127, but is somewhat hotter at the minima. We identify about 100 spectral lines in the $3700 - 7300$ Å wavelength range. As of today, our spectroscopy is the most comprehensive for this object. The velocity of the wind is derived using the He I triplet lines (360 ± 30 km s^{-1}). Physical parameters of the nebula around V532 are estimated.

Key Words: galaxies: individual (M33) — stars: individual (Romano's star) — stars: Wolf-Rayet — supergiants

1. INTRODUCTION

Luminous Blue Variables (LBVs) are a class of rare astrophysical objects introduced by Conti (1984) and remain a subject of intense interest. LBVs are broadly accepted to be very massive and energetic stars emitting close to the Eddington limit, evolving from Of toward Wolf-Rayet stars. However, contemporary evolutionary models do not answer the question about the exact relations between LBV, nitrogen-rich Wolf-Rayet (WN) and hydrogen-rich WN (WNH) stars. Numerical simulations show that the objects may pass the LBV evolutionary stage either before or after the WNH stage (Smith & Conti 2008). Currently, only 35 LBV and LBV candidates are known in our Galaxy (Clark, Larionov, & Arkharov 2005). Studying LBVs in nearby galaxies is very important for understanding stellar evolution and the evolution of the interstellar medium perturbed and contaminated by massive stars at various evolutionary stages.

The object V532 ($\alpha = 01^h35^m09.^s71$, $\delta = +30°41'57.''1$) is located in the outer spiral arm of the M33 galaxy. Giuliano Romano was the first to recover its light curve (Romano 1978) and to find irregular magnitude variations between $16.^m7$ and $18.^m1$. Romano classified V532 as a variable of the Hubble-Sandage type by the shape of the light curve and

[1]Stavropol State University, Russia.
[2]Special Astrophysical Observatory, Russia.
[3]Sternberg Astronomical Institute, Russia.

TABLE 1

OBSERVATIONAL LOG FOR MPFS DATA. S/N IS SIGNAL-TO-NOISE RATIO PER RESOLUTION ELEMENT

Date	Exposure time (s)	Seeing ($''$)	S/N	Spectral standard star	Spectral range (Å)
05 10 2002	900	3.8	16	BD25d4655	4250–6700
13 11 2004	4200	1.5	20	HZ44	4000–7000
17 01 2005	3600	1.5	18	G248	4000–7000

its colour index. Humphreys & Davidson (1994) on the basis of its light variations classified the star as an LBV candidate. Two maxima of brightness were detected during the last half of the century (Kurtev et al. 2001). The first was observed around 1970 and the second in the early 1990s (Kurtev et al. 2001). Long-term variability has an amplitude of about $1^{\rm m}$ and seems to be superimposed on an even stronger downward trend. Short-timescale variability with amplitude $\sim 0\overset{\rm m}{.}5$ was discovered in addition to the longer-timescale variability (Kurtev et al. 2001; Sholukhova et al. 2002). Such photometric behavior is typical for an LBV star.

The first optical spectrum was obtained by T. Szeifert (1996) at the 3.5 m Calar Alto telescope in 1992. In this spectrum, “few metal lines are visible, although a late B spectral type is most likely (faint HeI)”. This spectrum, obtained with the TWIN spectrograph of the Calar Alto telescope, is unique in being obtained in a profound flare state. It is drastically different from the hot spectra observed at the minima of brightness (see below).

Another spectrum was obtained by O. Sholukhova at the 6 m telescope of the Special Astrophysical Observatory (SAO) of the Russian Academy of Sciences (RAS) in 1994 (Sholukhova et al. 1997). Another spectrum was obtained at SAO with the Multi-Pupil Fiber Spectrograph (MPFS) in September 1998. This spectrum was classified as WN10–WN11 Fabrika et al. (2005). Polcaro et al. (2003) estimated the bolometric absolute magnitude of the object as $M_{\rm bol} \simeq -10\overset{\rm m}{.}4$, using a bolometric correction “of at least –3 mag” and the distance modulus $m - M = 24\overset{\rm m}{.}8$. They classify V532 as an LBV because the object fulfills all the criteria of Humphreys & Davidson (1994). Using five spectra obtained in 2003–2006, Viotti et al. (2006, 2007) find an anti-correlation between equivalent widths of the Wolf-Rayet blue bump at 4630–4686 Å and visual luminosity.

Comparing the spectra published by Szeifert (1996), Fabrika et al. (2005) and Viotti et al. (2007), we find that the object changes its spectral properties significantly.

Here we combine the spectral observations (both new and already published) with the light curve of the object to trace the spectral variability of the star. We describe the data and data reduction process in the next section. Results are presented in § 3 and discussed in § 4. In § 5, we present the conclusions.

2. OBSERVATIONS AND DATA REDUCTION

In this work, we use archival data from the 6m SAO telescope[4] and the SUBARU telescope, which is operated by the National Astronomical Observatory of Japan. The 6 m telescope data were obtained with the Multi Pupil Fiber Spectrograph (MPFS) (Afanasiev, Dodonov, & Moiseev 2001) and with the SCORPIO multi-mode focal reducer in the long-slit mode (Afanasiev & Moiseev 2005). The data from SUBARU were obtained with the Faint Object Camera (FOCAS) (Kashikawa et al. 2002) in the Cassegrain focus. Uncertainties are everywhere dominated by statistical Poissonian noise (readout noise and round-off errors are significantly smaller).

2.1. *MPFS Data*

MPFS obtains simultaneously the spectra from 240 (16×15) or 256 (16×16) spatial sampling elements arranged in the form of a rectangular array of square lenses. In 2002 and 2004–2005, the data were obtained in the 240-element and 256-element configurations, respectively. Spatial sampling of $1'' \times 1''$ was used. Light from individual sampling elements is collected by microlenses and transmitted by means of optical fibers reorganized in the form of a pseudo-slit toward the spectral camera. Grating # 4 (600 Å pix^{-1}) providing a spectral resolution of about 6 Å was used for all the observations. Detectors CCD TK 1024 (1024×1024 pixels) and EEV42-40 (2048×2048 pixels) were used in 2002 and 2004–2005, respectively. A sky background spectrum at a distance of $4''$ away from the

[4] Available via ASPID database `http://alcor.sao.ru/db/aspid/`.

TABLE 2

OBSERVATIONAL LOG FOR THE SCORPIO DATA. α IS SEEING, PA IS POSITION ANGLE, S/N IS SIGNAL-TO-NOISE RATIO

Date	Exposure time (s)	Grism	Spectral range (Å)	$\delta\lambda$ (Å)	S/N	$\alpha('')$	Spectral standard star	PA (°)
06 02 2005	600				8	1.7	G248	−136
30 08 2005	1200	VPHG550G	3500–7200	10	30	1.9	G191-B2B	210
08 11 2005	3300				45	1.9	BD25d4655	145
03 08 2006	1500				20	2	GD248	200
10 08 2007	1800	VPHG1200G	4000–5700	5	24	2	BD33d2642	252
05 10 2007	2700				40	1.1	BD25d4655	−141
08 01 2008	1800	VPHG1200R	5700–7500	5	20	2.1	BD25d4655	48
10 01 2008	1800	VPHG1200G	4000–5700	5	20	1.4	BD25d4655	18

object is taken simultaneously with the object by 17 (for 16×16 field size) or 16 (for 16×15 configuration) additional fibres. We summarize the relevant information on the MPFS data in Table 1.

The data reduction system was written in the IDL environment and makes use of procedures written by V. Afanasiev, A. Moiseev and P. Abolmasov. The reduction process consists of the standard steps for panoramic data reduction (see for example Sánchez 2006): bias subtraction, flat-fielding, removal of cosmic-ray hits, extraction of the individual spectra from the frames and their wavelength calibration using the spectrum of a He-Ne-Ar lamp. At every wavelength, we calculate the median sky level using the offset fibres and subtract from the spectra of the field. Spectra of spectrophotometric standard stars were used for absolute flux calibration.

Three emission-line spectra obtained with MPFS in 2002–2005 were used. We estimate the signal-to-noise ratio in continuum as 10–30 per resolution element (see Table 1 for details). Integral spectra were extracted in an annular aperture $2''$ in radius. Up to the instrumental resolution, the object is point-like. Note that, unlike long-slit spectrographs, MPFS being free from slit losses and absolute flux calibration, is much more reliable.

2.2. *SCORPIO Data*

Observational data from SCORPIO are summarized in Table 2. All the spectra were reduced using the `ScoRe` package for long-slit data reduction, written in IDL[5]. CCD frames were de-biased, cosmic

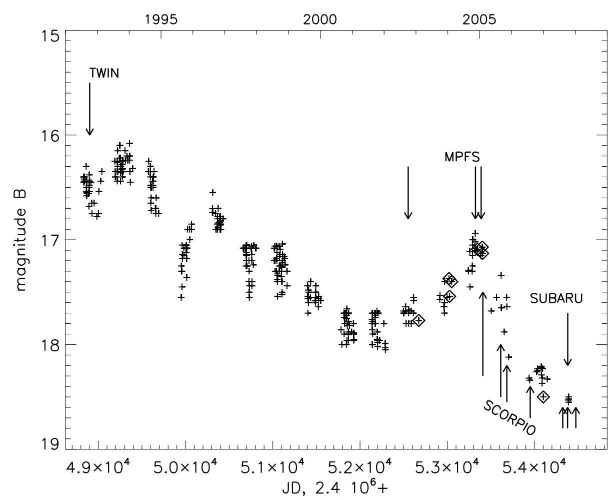

Fig. 1. *B*-band light curve of V532. Arrows indicate when spectroscopic observations were made. Data from (Viotti et al. 2007) are shown by diamonds.

particle hits were removed from all types of exposures except bias. Save for the single 10 minute long exposure obtained in February 2005, several object exposures are present for every day, which simplifies the removal of cosmic hits. Then we divide object and spectral standard exposures over the normalized mean flat-field frame. After wavelength calibration using He-Ar-Ne lamps and night sky OI (λ 5577 or λ 6300 depending on grism) emission lines, the CCD data were flux-calibrated using standard stars from Oke's (1990) spectrophotometric standard list (see Table 2). Spectra were extracted by fitting the profiles of slices across dispersion with a Gaussian function.

[5]Available at `http://narod.ru/disk/24196358000/Score_v1.2.tar.html`.

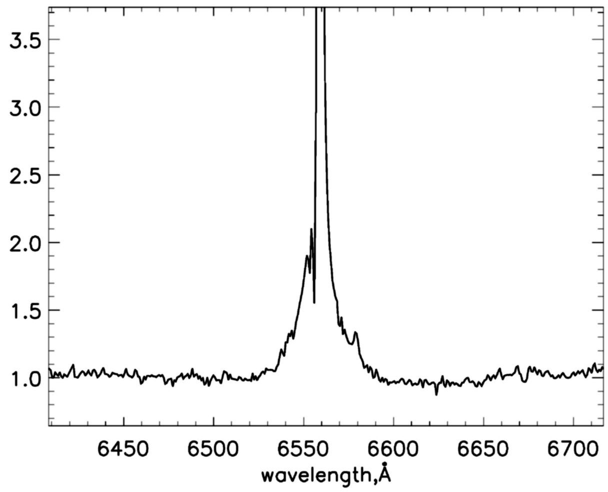

Fig. 2. Hα line profile in the Calar Alto spectrum obtained in 1992. The spectrum is normalized by the local continuum level.

In total, eight spectra were obtained with SCORPIO in 2005–2008 (dates of observations are shown by upward arrows in Figure 1). The spectral resolution is 10 Å (for VPHG550G grism) and 5 Å (for VPHG1200G and VPHG1200R grisms), the signal-to-noise ratios of the continuum vary from about 10 to about 50 for larger total exposures.

2.3. *Data from SUBARU*

One exposure 1200s in length was obtained with the SUBARU telescope on October 2007. The VPHG450 grism was used providing the spectral range of 3750–5250 Å. A slit width of 0.″5 implies a spectral resolution of about 1.7 Å (currently, it is the best resolution achieved for this object) in the extracted spectrum. Data were reduced using IDL-based software. The CCD frames were bias-subtracted and flat-fielded. We used the Th-Ar arc spectrum for wavelength calibration. Star BD40d4032 from the SUBARU spectrophotometric standard list was used to calibrate the stellar spectra. We extracted the spectrum in the same way we did for SCORPIO (see above § 2.2).

If we degrade the spectral resolution to 5 Å, the spectrum becomes practically identical to the spectrum obtained with SCORPIO on the same date. Though the spectral shapes are similar, the spectra differ in normalization (by about a factor of three) connected to slit losses.

2.4. *Photometric Data*

The light curve (see Figure 1) was provided by Vitalij Goranskij and consists of the CCD data obtained by Goranskij and Zharova with the 1 m SAO telescope and two instruments of the Crimean laboratory of the Sternberg Astronomical Institute (SAI), and photographic plates from the SAI collection. CCD data were reduced with MaxIm DL software[6]. The joint light curve will be published by A. V. Zharova et al. (in preparation) in a separate paper, all the details of the data reduction process will be given there. Photographic B-band magnitudes were identified with the B-band magnitudes obtained by CCD observations. CCD data uncertainties are of the order of 0.05 mag, plate data have larger errors depending on the source brightness, usually of the order 0.1–0.2 mag.

The joint curve contains the data of Viotti et al. (2007) but complements them with much larger photometric material and primarily allows to trace the recent evolution of the object.

3. RESULTS

3.1. *Spectral Evolution*

The first optical spectrum of V532 was obtained during the rise of brightness, when the object was $16^{\mathrm{m}}.4$ in the V band. This spectrum covers two spectral ranges $\lambda\lambda$ $4400 - 5000$ and $\lambda\lambda$ $5800 - 6750$, as it was obtained with the two-channel TWIN spectrograph[7]. In this spectrum, two strong lines are present, Hα (shown in Figure 2) and Hβ, having complex profiles consisting of a narrow line with P Cyg profile and broad wings. FWHM (Full Width at Half Maximum intensity) of the wings is $\sim$ 15 Å for Hβ and $\sim$ 20 Å for Hα. Such wings were first found for LBVs in the spectrum of P Cygni by Bernat & Lambert (1978). These wings are explained by scattering of line photons by free electrons in the stellar wind. Similar line profiles were observed for the LBV stars R127 and AG Car during the initial rise to maximum (Stahl et al. 1983, 2001).

Emission lines of He I λ 5876 and Si II λ 5957.612, 5978.970, 6347.091, 6371.359 are also present in the red spectrum. Szeifert (1996) mentions these SiII lines as “weak metal emissions”.

Figure 3 shows all the spectra of V532 in the blue range (4000–5500 Å) analysed in this article, obtained at different spectral resolutions. All the spectra are normalised to continuum level in a uniform way. In order to get a reasonable normalisation for our spectra, we chose several wavelength intervals practically free from Wolf-Rayet emissions (4250–4270, 5100–5200, 5520–5620, 5750–5800 and

[6] `http://www.cyanogen.com/maxim_main.php`.

[7] A comprehensive description is present at `http://www.caha.es/CAHA/Instruments/TWIN/HTML/twin.html`.

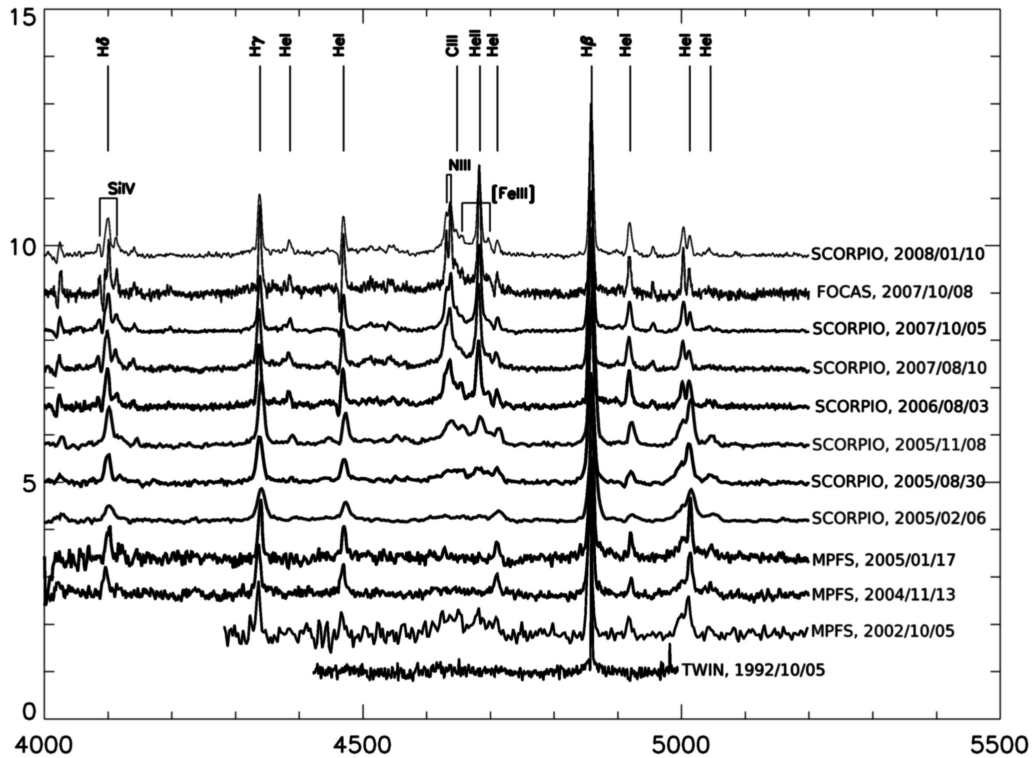

Fig. 3. Optical spectrum evolution in the blue spectral range (4000–5200 Å). Spectra are normalized by the local continuum level and vertically shifted for clarity.

TABLE 3

SPECTRAL CLASSES IDENTIFIED VIA THE SCHEME OF SMITH, CROWTHER, & PRINJA (1994)

B, mag	Spectral subtype	Date
17.5	WN10.5	2002/10/05
16.9	WN11	2004/11/13
17.1	WN11	2005/01/17
17.15	WN11	2005/02/06
17.3	WN10	2005/08/30
17.6	WN9	2005/11/08
18.3	WN8	2006/08/03
18.4	WN8	2007/08/10
18.5	WN8	2007/10/05–08
	WN8	2008/01/08–10

6950–6970 Å) and reconstructed the continuum using a second-order polynomial. Below, for spectral classification we use characteristic equivalent width ratios, which makes our results practically independent of spectral resolution.

The spectral appearance of the spectra of V532 obtained in 2002–2008 resembles that of late WN stars. It allows us to apply a classification scheme used for WN stars, bearing in mind that abundances of individual elements may differ, but physical conditions are similar. All the spectra obtained between 2002 and 2008 were classified using the classification of Smith, Crowther, & Prinja (1994) for WN6-11 stars based primarily on relative strengths of N V $\lambda\lambda$ 4604 − 20, N IV λ 4058, N III $\lambda\lambda$ 4634 − 41 and N II λ 3995 emission lines. The method has low dependence on elemental abundances, though only helium and nitrogen lines (preferably, ratios of the lines of one element) are used. The results of the spectral classification are given in Table 3.

The light curve exhibits a local maximum in 2004 and early 2005. In the spectra obtained in this period, one may observe strong emission lines of hydrogen and neutral helium. The spectral appearance of V532 shows strong similarities with a spectrum of a WN11 star. He I λ 4713 line is stronger than the N II blend, and He II λ 4686 is absent. In the spectrum obtained in 2002, the N II λ 3995 line is outside the spectral range; therefore we carry out the classification comparing N III $\lambda\lambda$ 4634 − 41 and

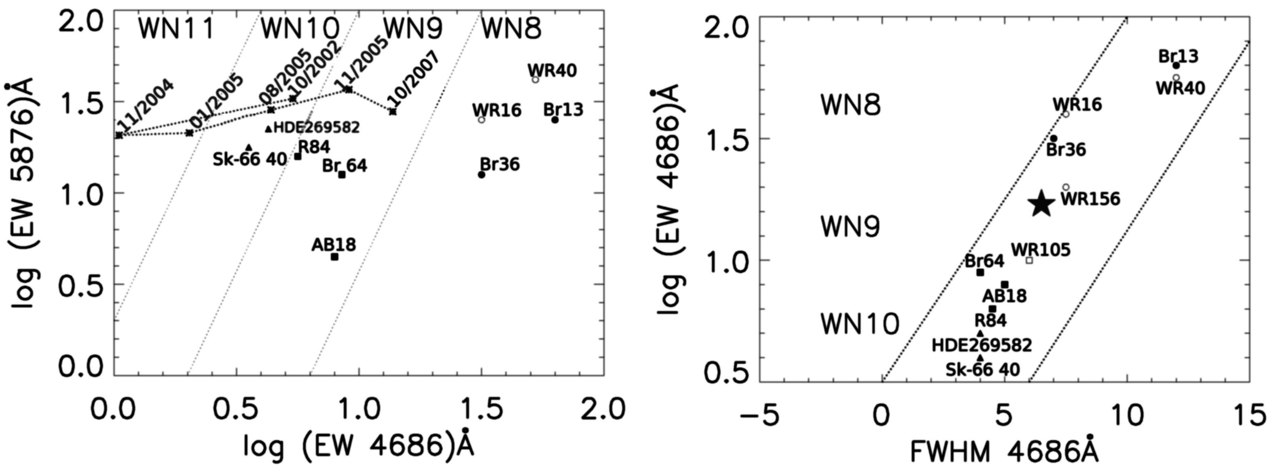

Fig. 4. Left panel: V532 location on the equivalent width diagram of He I λ 5876 versus He II λ 4686 for different dates of observation. The points are connected with dotted lines in chronological order. Right panel: V532 location in October 2007 (FOCAS data) on the equivalent width versus FWHM diagram for the He II λ 4686 line. In both graphs, known Galactic (open symbols) and LMC (filled) WN stars are shown for comparison: WN8 by circles, WN9 by squares, and WN10 by triangles. Data for these objects were taken from Smith et al. (1995).

N II $\lambda\lambda$ 4601 − 43 blends having similar intensity to the N II λ 3995 emission. N III $\lambda\lambda$ 4634 − 41 lines appear, but are weaker than N II $\lambda\lambda$ 4601 − 43. He II λ 4686 line is approximately as bright as the N II $\lambda\lambda$ 4634 − 41 emission; hence we classify the object as WN10.5.

Starting from the middle of 2005, Romano's star weakens in the optical range; its visible magnitude falls from 17 to $18^{\mathrm{m}}.8$. During this period its spectrum evolves from WN10 (August 2005) through WN9 (November 2005) to WN8 (August 2007) by three spectral sub-classes. In October 2007, He II λ 4686 line is stronger than N III $\lambda\lambda$ 4634 − 41. However, the N IV lines do not appear in the spectrum. We also classify the spectrum as WN8.

The evolution of V532 on the equivalent width diagram of He I λ 5876 versus He II λ 4686 is shown in the left panel of Figure 4. Locations of well-proven Galactic and Large Magellanic Cloud (LMC) Wolf-Rayet stars R84 (WN9), Sk-60 40 (WN10), LBV HDE 269582 (WN10) and some other objects are shown for comparison with our object. The figure shows that in the period between 2002 and 2005, when the star brightened by about one magnitude, its spectrum changed from WN9.5 to WN11. Since 2005, the spectrum has changed smoothly according to the sequence established by Smith, Shara, & Moffat (1996).

We used a quantitative chemistry-independent criterion based on the FWHM of the He II λ 4686 line for an alternative spectral classification. In Figure 4, we show the location of V532 on the diagram of the equivalent width of He II λ 4686 versus the FWHM of this line. We have measured equivalent width and FWHM of the He II line in the FOCAS spectrum. For this, we approximate the Wolf-Rayet blue bump by 7 Gaussians. The position of V532 is fully consistent with its Galactic and LMC WN9 analogues. The spectral class defined from the diagram is consistent with that determined from the relative strengths of N II, N III and He I with an accuracy of about one subclass.

Table 4 shows the lines detected in the spectra obtained with FOCAS (October 2007) and with SCORPIO (January 2008, with grisms 1200G and 1200R). Three spectra are used in order to cover the maximal wavelength range at maximal possible spectral resolution. The spectrum of V532 does not change noticeably from October 2007 to January 2008. Equivalent widths of the principal lines (absorptions, emissions and P Cyg) are given with errors of approximation. Uncertainties due to the choice of the continuum level are smaller than the errors of approximation. Lines with P Cygni profiles were resolved by fitting with the models described in the next subsection.

3.2. *Line Profiles and Terminal Wind Velocity*

In Figure 5 we show the FOCAS spectrum in the optical blue range 3800 − 5100 Å. The Wolf-Rayet blue bump (consisting primarily of N III $\lambda\lambda$ 4634, 4640, C III λ 4650, He II λ 4686 and He I λ 4713) is clearly seen in this spectrum.

TABLE 4

LIST OF EMISSION LINES DETECTED IN THE FOCAS AND SCORPIO (JANUARY 2008) SPECTRA OF V532[a]

λ, Å	Ion	EW emission Å	EW absorption Å	λ, Å	Ion	EW emission Å	EW absorption Å
3770.60	H11+HeII			4613.90	NII		
3797.90	H10+HeII			4621.40	NII		
3819.76	HeI			4630.54	NII		
3835.39	H9+HeII			4634.00	NIII	6.2 ± 1.0	
3871.82	HeI			4640.64	NIII	7.4 ± 0.5	
3889.05	H8+HeI	11 ± 1	3.7 ± 1.3	4643.09	NII		
3964.73	HeI			4650.16	C III	5.0 ± 0.5	
3970.08	Hϵ+HeII			4658.10	[FeIII]	2.5 ± 1.0	
3994.99	NII			4685.81	HeII	15.2 ± 0.2	
4009.00	HeI			4701.50	[FeIII]	2.9 ± 1.0	
4025.60	HeI+HeII	2.5 ± 0.5	1.2 ± 0.2	4713.26	HeI	1.6 ± 0.2	
4088.90	SiIV			4861.33	Hβ	22.5 ± 1.5	
4097.31	N III			4921.93	HeI	4.3 ± 0.2	
4101.74	Hδ+HeII	7.6 ± 1.0		4958.91	[O III]	1.3 ± 0.2	
4103.40	NIII			5006.84	[O III]	3.9 ± 0.6	
4116.10	SiIV			5015.67	HeI	2.6 ± 0.3	
4120.99	HeI			5411.50	HeII	6.2 ± 0.2	
4143.76	HeI			5666.60	NII		
4199.80	HeII			5676.02	NII		
4236.93	NII			5679.56	NII		
4241.79	NII			5686.21	NII		
4241.79	NII			5710.76	NII		
4340.47	Hγ+HeII	8.0 ± 0.3		5875.79	HeI	25.5 ± 0.7	
4387.93	HeI	1.4 ± 1.0		6548.00	[N II]		
4471.69	HeI	5.0 ± 0.3	1.7 ± 0.2	6562.82	Hα+HeII	107 ± 3	
4481.13	MgII			6583.00	[N II]		
4510.90	NIII			6678.15	HeI	18 ± 3	
4514.90	NIII			6683.20	HeII		
4518.20	NIII			7065.44	HeI	18 ± 3	
4523.60	NIII			7135.73	ArIII	3.2 ± 0.3	
4530.80	NIII			7281.35	HeI		
4534.60	NIII						
4541.60	HeII						
4547.30	NIII						
4601.50	NII						
4607.20	NII						

[a]For higher signal-to-noise ratios, equivalent widths (EW) are given. For lines with P Cyg profiles, we give both emission and absorption component EWs.

We suppose that the lines near 4658 and 4701 Å are nebular lines of [Fe III]. They cannot belong to C IV since C IV $\lambda\lambda$ 5812, 5801 lines are not present in the SCORPIO spectrum obtained simultaneously in October 2007.

Analyzing the FOCAS spectrum of V532, we found that triplet and singlet lines of HeI have different profiles (see Figure 6). Triplet lines of He I (λ 3889, 4025, 4471) show strong P Cyg profiles, while singlet lines (λ 3965, 4922, 5016) have

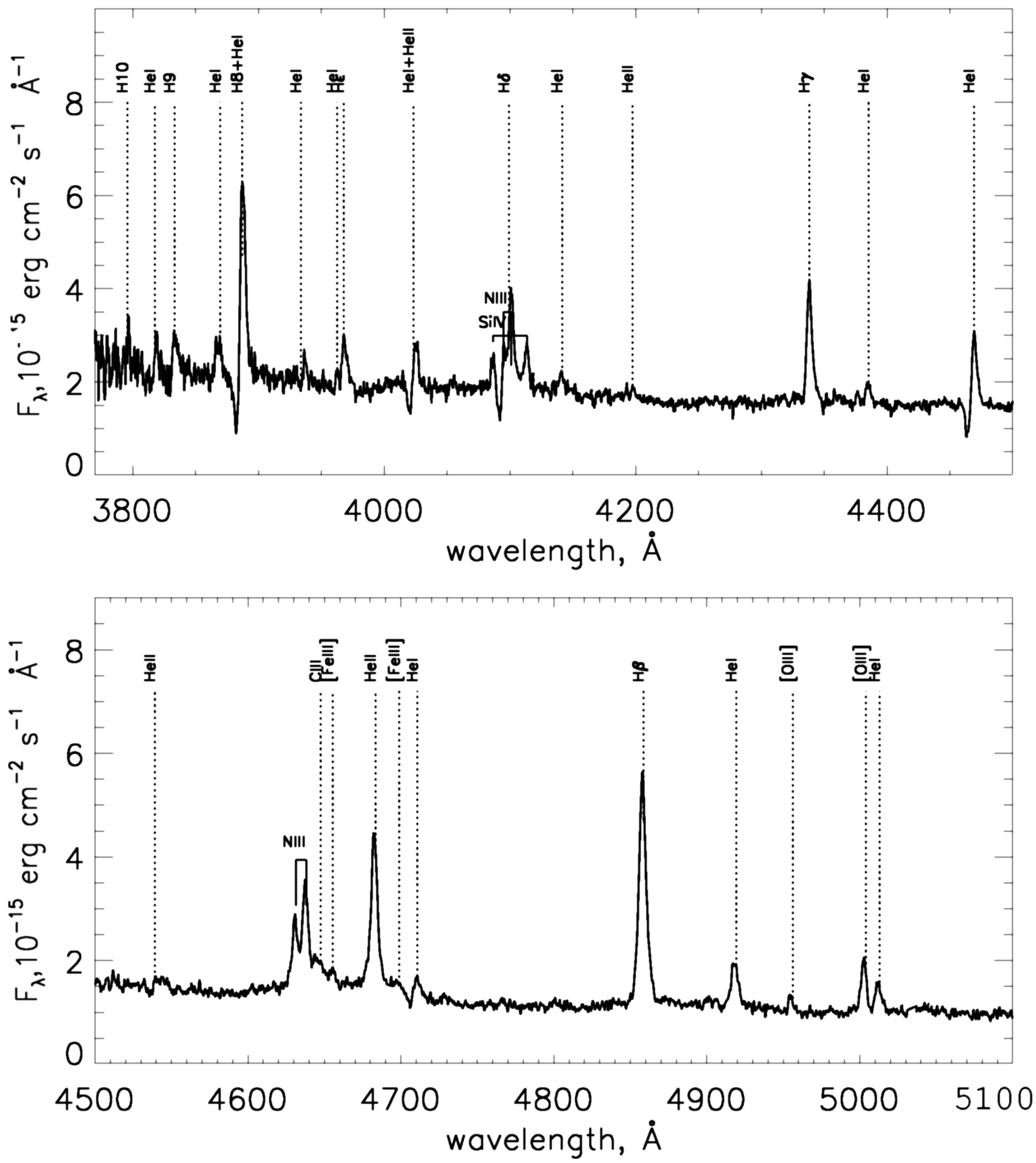

Fig. 5. Optical spectrum of V532 obtained with FOCAS in the range 3800–5100 ÅÅ.

flat-topped profiles. The widths of these lines correspond to a velocity span of about 100 km s^{-1}.

We used P Cyg profiles of triplet HeI lines to estimate the terminal wind velocity v_∞. Line profiles were fitted with a sum of two Gaussians (one representing the absorption, the other the emission component). We suppose that the widths of the emission and absorption components are equal to the instrumental profile width of 1.8 Å which is almost independent of wavelength. The instrumental profile width is determined using wavelength calibration spectrum lines of similar wavelengths. The terminal wind velocity is estimated by the velocity shift between the Gaussian centers. Even for the emission component of He I lines, we do not detect any Doppler broadening. This may mean that the profiles are not true P Cyg but wind blueshifted absorptions plus nebular emissions. This possibility does not however alter the wind velocity estimates.

Wind velocities for all the He I lines with P Cyg profiles are equal within the statistical errors. The mean wind velocity for the three triplet lines is 360 ± 30 km s^{-1}. This value is consistent with the terminal wind velocities for late WN (Crowther, Hillier, & Smith 1995; Smith, Crowther, & Willis 1995) which we give in Table 5 for comparison.

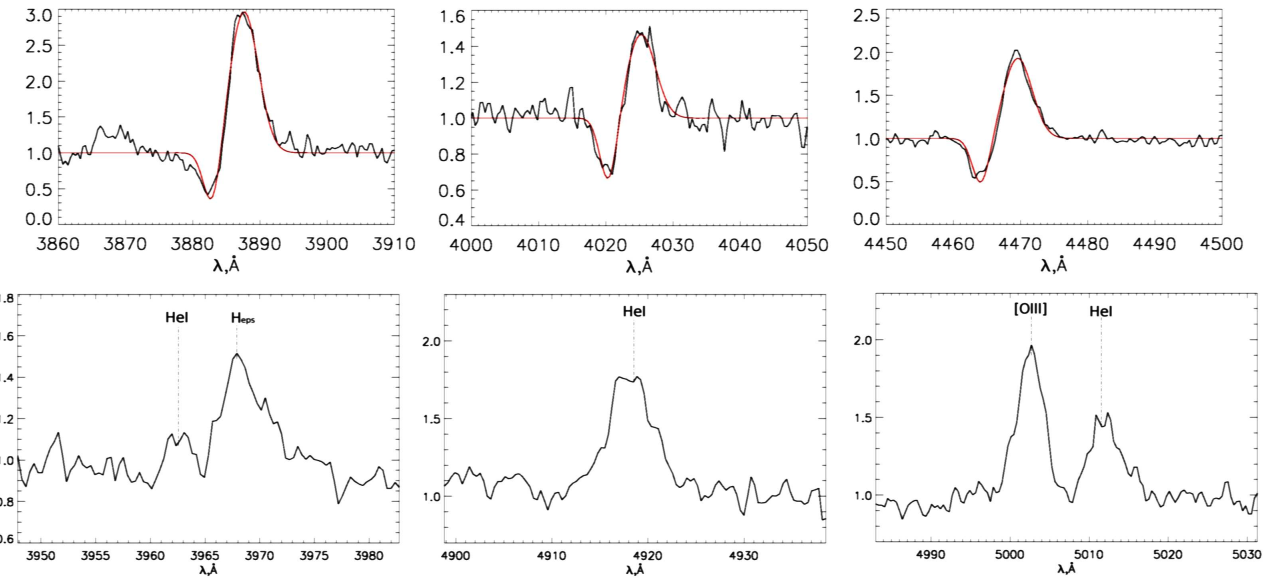

Fig. 6. Top panel: profiles of triplet He I λ 3889, 4025, 4471 lines (from left to right). Two-component model fits are shown (see text for details). Bottom panel: profiles of singlet He I λ 3965, 4922, 5016 lines. FOCAS data.

It is interesting to compare these profiles with the He II λ 5412 line in the SCORPIO spectrum obtained in October 2007. The spectrum has very high signal-to-noise ratio which allows reasonable terminal wind velocity estimates in spite of the significantly worse spectral resolution. The line has a classical low-optical-depth P Cyg profile: broad emission and blueshifted narrow absorption. We approximate this line by a classical P Cyg model profile (flat-topped emission with a narrow blueshifted absorption component) convolved with an instrumental point spread function that we consider Gaussian (the instrumental profile width is ~ 5.5 Å). Similar line profiles are produced by optically thin envelopes expanding at a constant velocity. Its fitting yields the wind speed of 200 ± 15 km s^{-1}. The expansion velocity indicates that the line is formed in the hotter inner parts of the wind that move with smaller outward velocities. Among Pickering emissions, we also detect λ 4541.6 and λ 4199.8 having similar profiles in the FOCAS spectrum, but we lack signal-to-noise to obtain reliable expansion velocity estimates for these lines.

3.3. *Nebular Lines*

The lines at 4959 and 5007 Å are clearly identified as [O III] emissions, which is consistent with their flux ratio equal to 3 and FWHMs equal within the measurement errors. In the cooler spectra of 2003 (Polcaro et al. 2003), nebular lines of [O III] are overridden by N II 4994-5005 emissions. However, in 2007, the N II lines are absent, but the [O III] λ 4959, 5007 doublet is clearly seen.

Nebular lines of [O III] $\lambda\lambda$ 4959, 5007, [N II] $\lambda\lambda$ 6548, 6583 are present in all the spectra analysed by us while the [S II] λ 6717, 6731 doublet is not. Therefore, we can estimate the electron density of the surrounding nebula. The electron density is between $10^{3.6}$ cm^{-3} and $10^{4.9}$ cm^{-3}. The former value corresponds to the critical density of the [S II] doublet, the second to that of [N II] $\lambda\lambda$ 6548, 6583 lines (see for example Osterbrock & Ferland 2006).

All the nebular lines present in the FOCAS spectrum as well as the [Ar III] λ 7135.73 emission in SCORPIO data show flat-topped or two-peaked profiles. The widths of the emission line cores are of the order of 100 km s^{-1}. Once we know the density of the emitting gas, we may estimate the size of the Strömgren region and the mass of the nebula surrounding V532. The former may be found as follows (see for example Lang 1974):

$$R_{\rm s} \simeq \left(\frac{3S}{4\pi\alpha n_{\rm e}^2}\right)^{1/3},$$

where α is the Case B recombination coefficient for hydrogen, $\alpha \simeq 2.6 \cdot 10^{-13} \left(\frac{10^4}{T}\right)^{0.85}$ cm^3 s^{-1}, $n_{\rm e}$ is the electron density, and S is the hydrogen-ionizing quanta production rate. For O9.5Ia stars, probably similar to the object in mass and luminosity, S is estimated as $10^{49.17}$ s^{-1} (Osterbrock & Ferland 2006).

TABLE 5

WIND VELOCITIES ESTIMATED THROUGH OPTICAL HEI LINES AND AMBIENT OXYGEN ABUNDANCES

Star	Galaxy	WN subtype	v_∞ km s^{-1}	$12+\log$ O/H abundance	HII region
V532 (during minimum epoch 2007)	M33	9	360	8.26 ± 0.08	
MCA1-B[a]	M33	9	420	8.315 ± 0.061	NGC588[e]
B517[b]	M33	11	275	8.334 ± 0.083	MA2[e]
Sk-66°40[a]	LMC	10	300		
R84[a]	LMC	9	400		
BE381[c]	LMC	9	280	8.37	30 Dor[f]
WR105[a]	MW	9	700		
AG Car (during minimum epoch 1985–1990)[d]	MW	11	300		
AG Car (during minimum epoch 2002)[d]	MW	11	200		

[a]Smith et al. (1995). [b]Crowther et al. (1997). [c]Crowther et al. (1995). [d]Groh et al. (2009). [e]Rosolowsky & Simon (2008). [f]Rosa & Mathis (1987).

One may estimate the size of a homogeneous nebula around V532 as:

$$R_{\rm s} \simeq 0.1 \cdot \left(\frac{S}{10^{49}{\rm s}^{-1}}\right)^{1/3} \times \left(\frac{n_{\rm e}}{10^4~{\rm cm}^{-3}}\right)^{-2/3} \times \times \left(\frac{T}{10^4{\rm K}}\right)^{0.28} {\rm pc}\,. \quad (1)$$

Note that possible inhomogeneity has little effect on the linear size: for a gas filling only some part of the nebular volume f, $R_{\rm s}$ should scale with filling factor as $\propto f^{-1/3}$. However, sizes of about 1 pc are plausible. The nebular mass may be trivially inferred as:

$$M \simeq \rho \cdot \frac{4\pi}{3} R_{\rm s}^3$$

$$\simeq 0.17 \cdot \left(\frac{S}{10^{49}{\rm s}^{-1}}\right) \left(\frac{n_{\rm e}}{10^4~{\rm cm}^3}\right)^{-1} \left(\frac{T}{10^4{\rm K}}\right)^{0.84} \cdot M_\odot\,. \quad (2)$$

The estimated size and the ionised mass of the nebula are consistent with these for ejecta of LBV stars (see Smith et al. 1994, and references therein) to order of magnitude. It is possible that the total mass lost by the object is higher, about several solar masses, but we observe only the ionized part of the envelope. The emitting gas was probably ejected during one or several outburst events at wind velocities of about 100 km s^{-1}.

4. DISCUSSION

In Table 5, terminal wind velocities for the WN9-WN11 stars in the Galaxy, LMC and M33 and LBV star AG Car (during minimum) are given. These velocities are also estimated through the optical He I lines. Because wind acceleration is tightly connected to metallicity (Massey et al. 2004; Puls, Vink, & Najarro 2008), we also give oxygen abundances ($12 + \log$ O/H) for selected H II regions adjacent to MCA1-B, B517 and BE381. They may be used as a measure for initial object metallicities.

V532 is located at a distance of about 17′ from the centre of M33. Taking the central oxygen abundance value of $12+\log {\rm O/H} = 8.36 \pm 0.04$ and a radial gradient of -0.027 ± 0.012 dex kpc^{-1} (Rosolowsky & Simon 2008), we may estimate the primordial oxygen abundance for V532 as 8.26 ± 0.08. The ambient metallicity is thus similar to that of the 30 Dor star-forming region. Our estimate for the terminal wind velocity of V532 is fairly consistent with that of other late WN stars in similar environments.

Wolf-Rayet stars are believed to be more evolved objects than Ofpe and Be supergiants. Information on elementary abundances may cast some light upon this issue. However, to recover reliable abundance estimates, one needs sophisticated modelling of both the moving atmosphere of the star and its structure. Here, we restrict ourselves only to some semi-qualitative estimates for the H/He abundance ratio. We compare the equivalent width ratios of Hβ to he-

TABLE 6

EQUIVALENT WIDTHS OF HELIUM LINES (IN Hβ UNITS) AND HELIUM-TO-HYDROGEN ABUNDANCE RATIOS FOR TWO LATE HYDROGEN-RICH WNS AND V532 (2007)

Object	Spectral Class	H/He	He I+H8 3889	Hγ	He II 4686	He I 4713	He I 5876
R84	WN9	2.5	3	2.3	3.5	12.6	
BE381	WN9h	2	2.1	2.4	1.9	16.6	0.8
V532			2	2.75	1.4	13.4	0.8

lium lines in the spectra obtained in 2007 to those for several WN9 (taken from Crowther et al. 1995) to estimate the relative abundances of hydrogen and helium. The equivalent width ratios are given in Table 6. The table shows that they are similar to those for BE381 (Brey 64) that has H/He=2 and is classified as WN9h by Crowther & Smith (1996). By analogy with BE381, we suppose that for V532, H/He $\sim$ 2. It places Romano's star in the region occupied by hydrogen-rich late WN stars that have atmospheres moderately contaminated by helium.

We have already mentioned the strikingly diverse behaviour of triplet lines of He I having P Cyg-like profiles and singlet emissions. Probably singlet lines have weak absorptions that we cannot detect due to insufficient signal-to-noise or spectral resolution. Besides this, He I λ 5015 is contaminated by the oxygen [O III] λ 5007 emission.

The similarity of the line profiles of singlet He I, [O III] $\lambda\lambda$ 4959, 5007 and [Ar III] λ 7136 suggests that both singlet He I and forbidden emissions are produced mainly in the low-density ejecta, expanding at velocities of about 100 km s^{-1}. Probably, singlet and triplet lines of neutral helium are formed in different places. Because the lowest possible level for triplet lines is metastable, concentrations of atoms at the lower levels of triplet transitions (and therefore the intensities of absorption line components) should be higher.

We classify the observed evolution of the object as an S Dor variability cycle. The main difference from AG Car and other LBVs is that at the optical minimum V532 becomes much hotter and may be classified as a WN9/WN8 star, while AG Car stops at about WN11. The non-monotonous spectral changes and variability timescales indicate that these spectral changes hardly correspond to any real stellar evolution, rather being connected to the ordinary LBV variability. It also means that LBV stars may have spectral classes as early as WN8. To our notion, there is only one example of an object that acquired even earlier spectral classes of WN6/7 during LBV variability cycle, HD5980 (Barbá, Niemela, & Morrell 1997; Koenigsberger & Moreno 2008) in the SMC. The hot spectra of this object are probably connected to lower ambient metallicity, too.

V532 is one more example of an LBV star temporarily becoming a WN. We predict that, vice versa, some of the Galactic or extra-galactic Wolf-Rayet stars may prove to be dormant LBVs. Probably, the hottest possible temperature for an LBV decreases with metallicity, but more data on the brightest stars in different environments are needed.

5. CONCLUSIONS

Our results show that the object changes from a *B* emission line supergiant at optical maximum, through Ofpe/WN (WN10,WN11) to WN9 and further towards a WN8 star at deep minimum. We confirm the result of Viotti et al. (2007) that there is an anti-correlation between the visual luminosity and the temperature of the star, with a larger amount of spectral data.

V532 spans a large range of spectral classes, becoming one of the first (probably, the second, after HD5980) LBV stars noticed to make an excursion as deep as WN8 into the Wolf-Rayet domain. It is interesting to trace further the evolution of the object. Further monitoring of V532, as well as of other late WN stars, is necessary to establish the evolutionary link between WRs and LBVs. Some WNs may prove to be dormant LBVs.

We are grateful to Vitalij Goranskij, Elena Barsukova and Alla Zharova for providing us with photometric data and Olga Sholukhova and Thomas Szeifert for the spectrum obtained with TWIN Calar Alto spectrograph in 1992. We would also like to thank the anonymous referee for valuable comments and for drawing our attention to HD5980.

REFERENCES

Afanasiev, V. L., Dodonov, S. N., & Moiseev, A. V. 2001, in Stellar Dynamics: From Classic to Modern, ed. L. P. Osipkov & I. I. Nikiforov (St. Petersburg: St. Petersburg Univ. Press), 103
Afanasiev, V., & Moiseev, A. 2005, Astron. Lett., 31, 194
Barbá, R. H., Niemela, V. S., & Morrell, N. I. 1997, in ASP Conf. Ser. 120, Luminous Blue Variables: Massive Stars in Transition, ed. A. Nota & H. Lamers (San Francisco: ASP), 238
Bernat, A. P., & Lambert, D. L. 1978, PASP, 90, 520
Clark, J. S., Larionov, V. M., & Arkharov, A. 2005, A&A, 435, 239
Conti, P. S. 1984, in IAU Symp. 105, Observational Tests of the Stellar Evolution Theory, ed. A. Maeder & A. Renzini (Dordrecht: Reidel), 233
Crowther, P. A., Hillier, D. J., & Smith, L. J. 1995, A&A, 293, 172
Crowther, P. A., & Smith, L. J. 1996, A&A, 305, 541
Crowther, P. A., Szeifert, Th., Stahl, O., & Zickgraf, F.-J. 1997, A&A, 318, 543
Fabrika, S., Sholukhova, O., Becker, T., Afanasiev, V., Roth, M., & Rossi, C. 2005, A&A, 437, 217
Groh, J. H., Hillier, D. J., Damineli, A., Whitelock, P. A., Marang, F., & Rossi, C. 2009, ApJ, 698, 1698
Humphreys, R., & Davidson, K. 1994, PASP, 106, 1025
Kashikawa, N., et al. 2002, PASJ, 54, 819
Koenigsberger, G., & Moreno, E. 2008, RevMexAA (SC), 33, 108
Kurtev, R., Sholukhova, O., Borrisova, J., & Georgiev, L. 2001, RevMexAA, 37, 57
Lang, K. R. 1974, Astrophysical Formulae (New York: Springer-Verlag)
Massey, P., Bresolin, F., Kudritzki, R. P., Puls, J. R., & Pauldrach, A. 2004, ApJ, 608, 1001
Oke, J. B. 1990, AJ, 99, 1621
Osterbrock, D. E., & Ferland, G. J. 2006, Astrophysics of Gaseous Nebulae and Active Galactic Nuclei (2nd ed.; Sausalito: University Science Books)
Polcaro, V. F., Gualandi, R., Norci, L., Rossi, C., & Viotti, R. 2003, A&A, 411, 193
Puls, J., Vink, J., & Najarro, F. 2008, A&AR, 16, 209
Romano, G. 1978, A&A, 67, 291
Rosa, M., & Mathis, J. S. 1987, ApJ, 317, 163
Rosolowsky, E., & Simon, J. D. 2008, ApJ, 675, 1213
Sánchez, S. F. 2006, Astron. Nachr., 327, 850
Sholukhova, O. N., Fabrika, S. N., Vlasyuk, V. V., & Burenkov, A. N. 1997, Astron. Lett., 23, 458
Sholukhova, O., Zharova, A., Fabrika, S., & Malinovskii, D. 2002, in ASP Conf. Proc. 259, Radial and Nonradial Pulsations as Probes of Stellar Physics, ed. C. Aerts, T. R. Bedding, & J. Christensen-Dalsgaard (San Francisco: ASP), 522
Smith, N., & Conti, P. 2008, ApJ, 679, 1467
Smith, L. J., Crowther, P. A., & Prinja, R. K. 1994, A&A, 281, 833
Smith, L. J., Crowther, P. A., & Willis, A. J. 1995, A&A, 302, 830
Smith, L. F., Shara, M. M., & Moffat, F. J. 1996, MNRAS, 281, 163
Stahl, O., Wolf, B., Klare, G., Cassatella, A., Krautter, J., Persi, P., & Ferrari-Toniolo, M. 1983, A&A, 127, 49
Stahl, O., et al. 2001, A&A, 375, 54
Szeifert, T. 1996, in Wolf-Rayet Stars in the Framework of Stellar Evolution, ed. J. M. Vreux, A. Detal, D. Fraipont-Caro, E. Gosset, & G. Rauw (Liege: Univ. Liege-Institute d'Astrophysique), 459
Viotti, R. F., Galleti, S., Gualandi, R., Montagni, F., Polcaro, V., Rossi, C., & Norci, L. 2007, A&A, 464, L53
Viotti, R. F., Rossi, C., Polcaro, V. F., Montagni, F., Gualandi, R., & Norci, L. 2006, A&A, 458, 225

O. Maryeva: Stavropol State University, Pushkina Str., 1, Stavropol, Russia 355009, Russia and Special Astrophysical Observatory, Nizhnij Arkhyz, Zelenchukskij, Karachai-Cirkassian Republic, Russia 369167 (olga.maryeva@gmail.com).

P. Abolmasov: Sternberg Astronomical Institute, Moscow State University, Universitetsky pr., 13, Moscow 119992, Russia (pavel.abolmasov@gmail.com).